

Improving Gradient-Trend Identification: Fast-Adaptive Moment Estimation with Finance-Inspired Triple Exponential Moving Average

Roi Peleg, Teddy Lazebnik, Assaf Hoogi

Abstract—The performance improvement of deep networks significantly depends on their optimizers. With existing optimizers, precise and efficient recognition of the gradients trend remains a challenge. Existing optimizers predominantly adopt techniques based on the first-order exponential moving average (EMA), which results in noticeable delays that impede the real-time tracking of gradients trend and consequently yield sub-optimal performance. To overcome this limitation, we introduce a novel optimizer called fast-adaptive moment estimation (FAME). Inspired by the triple exponential moving average (TEMA) used in the financial domain, FAME leverages the potency of higher-order TEMA to improve the precision of identifying gradient trends. TEMA plays a central role in the learning process as it actively influences optimization dynamics; this role differs from its conventional passive role as a technical indicator in financial contexts. Because of the introduction of TEMA into the optimization process, FAME can identify gradient trends with higher accuracy and fewer lag issues, thereby offering smoother and more consistent responses to gradient fluctuations compared to conventional first-order EMA. To study the effectiveness of our novel FAME optimizer, we conducted comprehensive experiments encompassing six diverse computer-vision benchmarks and tasks, spanning detection, classification, and semantic comprehension. We integrated FAME into 15 learning architectures and compared its performance with those of six popular optimizers. Results clearly showed that FAME is more robust and accurate and provides superior performance stability by minimizing noise (i.e., trend fluctuations). Notably, FAME achieves higher accuracy levels in remarkably fewer training epochs than its counterparts, clearly indicating its significance for optimizing deep networks in computer-vision tasks.

Index Terms—Deep Learning Optimization, Exponential Moving Average, Trend Tracking.

I. INTRODUCTION

MODERN deep learning relies heavily on the efficacy of optimization algorithms, and the advent of improved optimization techniques has had profound and wide impacts on the field of deep learning [1]. Two main branches of first-order optimization methods are widely used for training deep neural networks: the stochastic gradient descent (SGD) family and adaptive learning-rate methods. SGD scales the gradients uniformly in all directions [2]. Introducing Momentum into SGD enables a smoother descent and faster convergence by accumulating gradients from past data points [3]. Despite

its effectiveness and well-tuned learning rates, SGD requires considerable computation. To address this issue, adaptive first-order methods compute the individual learning rates for each parameter, which usually leads to faster convergence. Notable examples of adaptive optimization methods are *AdaDelta* [4], which uses a moving window of past gradient updates for a local view, and *AdaGrad*, which dynamically incorporates the knowledge of data geometry by normalizing gradients with past gradient magnitudes [5]. These methods provide good performance in various scenarios such as sparse data or data with small gradients. However, *AdaGrad* may suffer from diminishing learning rates over time. To overcome this problem, *RMSProp* [6] has been developed. *RMSProp* uses an exponentially decaying moving average over gradient magnitudes instead of the sum of the gradient magnitudes. The popular optimizer *Adam* builds upon *RMSProp* and uses an exponential moving average (EMA) over past gradients rather than relying solely on the current normalized gradient [7]. Variants of *Adam*, such as *AMSGrad* [8], *AdaBound* [9], *AdamW* [10], and *AdaHessian* [11], with further improved performance have been developed.

Several studies have explored the fusion of SGD and *Adam* to achieve fast convergence and generalization. An example is the *SWATS* joint framework [12], which switches from *Adam* to SGD. However, both *Adam* and SGD outperformed *SWATS*. Another proposed optimizer, *Mixing Adam and SGD (MAS)*, integrates SGD and *Adam* by weighting their contributions [13]. Although this idea is intriguing, the linear combination of *Adam* and SGD in *MAS* using *constant factors* yields limited performance improvement. **Notably, a prominent limitation of all the existing optimizers based on the first-order EMA is their pronounced delay in identifying data trends. This lag makes them extremely slow trackers, leading to sub-optimal performance.**

II. RELATED WORK

A. Identifying Trends

Despite extensive efforts to bridge the generalization gap between SGD variants and adaptive methods, this disparity persists [14]. A critical shortcoming of existing adaptive methods is their limited ability to adapt effectively and quickly to data trends during the optimization process. *Maiya et al.* introduced the *Trend over Momentum (Tom)* optimizer for computer-vision tasks.

R. Peleg and A. Hoogi are with the Department of Computer Science, Ariel University. Corresponding E-mail: assafh@ariel.ac.il
Teddy Lazebnik is with the Department of Mathematics, Ariel University and Cancer Institute, University College London University

This optimizer uses Holt’s linear trend model as a time-series model to predict the gradient trends [15]. By leveraging the gradient rate of change between successive time steps, Tom introduced a trend component to enhance convergence. However, its drawback is that it assumes persistent seasonal gradient trends, which may not be true in real-world scenarios. Notably, in the finance domain, Kolkova et al. demonstrated that technical indicators typically outperform Holt’s smoothing when identifying trends in seasonality-free financial data [16]. To address this limitation, our proposed approach aims to enhance adaptive methods by integrating a powerful technical indicator into the optimization process. By adopting this solution, adaptive methods become more responsive to trend changes during the optimization process, leading to improved performance and better adaptation to real-world data dynamics.

B. Exponential Moving Average (EMA)

EMA, or Exponential Moving Average, stands as a key tool within data modeling and time-series analysis. Its distinct advantage lies in the application of exponentially decreasing weights to past data, effectively smoothing out short-term fluctuations. Unlike traditional methods like Gaussian smoothing, EMA minimizes lag significantly. This is achieved by its inherent prioritization of recent data points in calculations, assigning them higher weights. Consequently, EMA adapts swiftly to changes in data, outpacing other methods that treat all data points equally. EMA’s rapid adjustment capability finds extensive use in stochastic optimizers, particularly in denoising data during optimization processes. This unique feature makes EMA a favored choice in scenarios where quick adaptation to changing data dynamics is crucial.

Let $x = x_{1:t}$ denote a data sequence up to time t . Then, EMA combines recursively the current and previous data values by

$$\begin{aligned} \text{EMA}(x_{1:t}) &= \beta \cdot \text{EMA}(x_{1:t-1}) + (1 - \beta) \cdot x_t \\ &= (1 - \beta) \sum_{i=0}^t \beta^i x_{t-i}, \end{aligned} \quad (1)$$

where $0 \leq \beta \leq 1$ is the smoothing hyper-parameter to be tuned; β determines the responsiveness of EMA to changes in the data, where lower values lead to a quicker response but with less effective denoising.

Two extensions of the standard EMA are the double exponential moving average (DEMA) and triple exponential moving average (TEMA). DEMA and TEMA were first introduced in the field of finance as technical indicators for evaluating trends in stock prices [17]. These higher-order extensions of EMA are powerful tools that combine the benefits of both *noise reduction* and *trend identification* by adding lag-correcting terms to the standard EMA estimation.

III. MAIN CONTRIBUTIONS

The major contributions of this study are as follows:

- **High-order EMAs:** To the best of our knowledge, our proposed fast-adaptive moment estimation (FAME) optimizer is **the first to leverage the great potential of**

higher-order EMAs for improved optimization, and it **overcomes the limitations of the first-order EMAs**, such as inherent lag and insufficient adaptation to data trends.

- **Inspired by TEMA used in the field of Finance: We incorporated TEMA**, which is widely used in the field of finance, as our high-order EMA. TEMA was originally used as a technical indicator in the stock market.
- **Active Guidance in Optimization:** In finance, TEMA is used as a *passive indicator*, and it is compared with market changes *but does not* directly affect them. However, **in our FAME optimizer, TEMA actively guides the optimization process and affects the network weights**. Thus, its applicability and usefulness are extended to high-dimensional optimization problems.
- **Data- and task-agnostic characteristics: FAME has proven to be data-agnostic and task-agnostic**. We conducted extensive evaluations using various datasets, architectures, and computer-vision tasks. The FAME was evaluated on six datasets using 15 architectures. Additionally, it was thoroughly compared with six optimizers. Across almost all evaluations, FAME consistently showed **improvements in performance accuracy, robustness, and number of required epochs**.

IV. PROPOSED FAME OPTIMIZER

In this section, we introduce our FAME optimizer (see Algorithm 1 for an outline). FAME provides a remarkably precise estimation of both the first- and second-order gradients (m_t, v_t), resulting in better gradient estimations than the original first-order EMA. The distinguishing feature of FAME lies in its ability to curtail lag during gradient moment estimation while concurrently delivering efficient denoising of these gradient trends.

Algorithm 1: Proposed FAME optimizer

Input: Hyper-parameters - $\beta_1, \beta_2, \beta_3, \beta_4, \beta_5, \alpha, \epsilon$

Output: Set of $\hat{\theta}_t$ parameters after convergence

```

1 Initialization :  $m_0 \leftarrow 0, v_0 \leftarrow 0$  ;
2 while  $\theta_t$  not converged do
3    $t \leftarrow t + 1$  ;
4    $m_t = \beta_1 m_{t-1} + (1 - \beta_1) g_t$  ;
5    $dm_t = \beta_3 dm_{t-1} + (1 - \beta_3) m_t$  ;
6    $tm_t = \beta_5 tm_{t-1} + (1 - \beta_5) dm_t$  ;
7    $m_{FAME_t} = 3m_t - 3dm_t + tm_t$  ;
8    $v_t = \beta_2 v_{t-1} + (1 - \beta_2) g_t^2$  ;
9    $dv_t = \beta_4 dv_{t-1} + (1 - \beta_4) v_t$  ;
10   $tv_t = \beta_4 tv_{t-1} + (1 - \beta_4) dv_t$  ;
11   $v_{FAME_t} = 3v_t - 3dv_t + tv_t$  ;
12   $\theta_t = \theta_{t-1} - \alpha \cdot \frac{m_{FAME_t}}{v_{FAME_t} + \epsilon}$ 
13 end
14 return  $\theta_t$ 

```

A. Higher-Order EMA

Although the simple EMA in Eq. (1) denoises the data, it also introduces a lag in the estimation (see Fig. 1), which may result in inadequate gradient updates and sub-optimal performance. When using DEMA, to reduce the lag, $\text{DEMA}(x)$ adds a lag-correcting term to $\text{EMA}(x)$

$$\begin{aligned} \text{EMA}(x - \text{EMA}(x)) &= \text{EMA}(x) - \text{EMA}(\text{EMA}(x)) \\ &= \text{EMA}_1(x) - \text{EMA}_2(x), \end{aligned} \quad (2)$$

where in the first equality, we used the linearity of EMA, and in the second equality, we introduced the notation

$$\text{EMA}_k(x) = \underbrace{\text{EMA}(\text{EMA}(\dots \text{EMA}(x)))}_{k \text{ times}}$$

for the recursive application of EMA on x for k times. The lag-correcting term in Eq. (2) is a smooth estimation of the true (but noisy) lag between the true data x and the naive smooth estimator $\text{EMA}(x)$, as measured from their difference $x - \text{EMA}(x)$. By adding the correction term in (2) to $\text{EMA}(x)$ we obtain DEMA,

$$\text{DEMA}(x) = 2\text{EMA}_1(x) - \text{EMA}_2(x). \quad (3)$$

One can go further and consider a lag correction to the first lag correction in (2), namely,

$$\begin{aligned} &(\text{EMA}_1(x) - \text{EMA}_2(x)) - \text{EMA}(\text{EMA}_1(x) - \text{EMA}_2(x)) \\ &= \text{EMA}_1(x) - 2\text{EMA}_2(x) + \text{EMA}_3(x). \end{aligned} \quad (4)$$

Adding the terms in (4) to DEMA in (3) gives TEMA,

$$\text{TEMA}(x) = 3\text{EMA}_1(x) - 3\text{EMA}_2(x) + \text{EMA}_3(x). \quad (5)$$

Fig. 1a shows the advantage of TEMA over EMA in identifying trends by responding more quickly to rapid changes in the data. Fig. 1b shows TEMA and EMA and the individual lag-correcting terms that comprise TEMA. Each term causes different lag reductions (i.e., different phases), and by adding all the terms, lagging is reduced drastically while maintaining the overall trend smoothness.

B. FAME Optimizer

Let $f(\theta)$ be a differentiable stochastic scalar function that depends on the parameters θ . It is a noisy version of the expected objective function $F(\theta) = \mathbb{E}[f(\theta)]$. The goal is to minimize $F(\theta)$ w.r.t. its parameters θ given only a sequence $f_1(\theta), \dots, f_T(\theta)$ of realizations of the stochastic function f at subsequent time steps $1, \dots, T$. The stochasticity in f may originate from the evaluation at random subsamples of data points instead of the entire data, or from inherent function noise. The gradient, i.e., the vector of partial derivatives of f_t w.r.t. θ , evaluated at time step t , is denoted by

$$g_t = \nabla_{\theta} f_t(\theta). \quad (6)$$

Similar to Adam, FAME tracks the first-order and second-order moments (m_t, v_t) of the gradients as estimated by an EMA_1 ,

$$\begin{aligned} m_t &= \beta_1 m_{t-1} + (1 - \beta_1) g_t, \\ v_t &= \beta_2 v_{t-1} + (1 - \beta_2) g_t^2, \end{aligned} \quad (7)$$

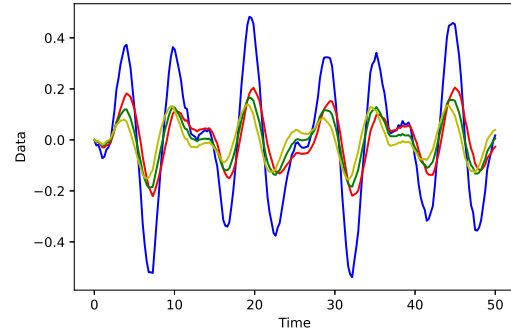
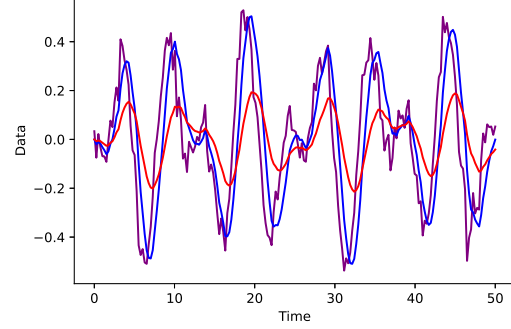


Fig. 1: **Upper-** Simulated demonstration of gradient trend estimation and lagging. Ground truth (GT, purple), triple exponential moving average (TEMA)-based estimation (blue), and exponential moving average (EMA)-based estimation (red). **Lower-** Demonstration of TEMA (blue) and its components, namely, $\text{EMA} = \text{EMA}_1$ (red) and its individual lag correction terms $(\text{EMA}_1 - \text{EMA}_2)$ (green) and $(\text{EMA}_1 - 2\text{EMA}_2 + \text{EMA}_3)$ (yellow); adding all terms according to the TEMA formulation $(3\text{EMA}_1(x) - 3\text{EMA}_2(x) + \text{EMA}_3(x))$ in blue. Further explanation is provided in Section IV in this paper.

where the hyper-parameters $\beta_1, \beta_2 \in [0, 1)$ control the exponential decay rates of these moving averages.

Based on the values of (m_t, v_t) , FAME additionally keeps track of the variables (dm_t, dv_t) for estimating EMA_2 ,

$$\begin{aligned} dm_t &= \beta_3 dm_{t-1} + (1 - \beta_3) m_t, \\ dv_t &= \beta_5 dv_{t-1} + (1 - \beta_5) v_t. \end{aligned} \quad (8)$$

Based on the values of (dm_t, dv_t) , the variables (tm_t, tv_t) track the estimation of EMA_3 ,

$$\begin{aligned} tm_t &= \beta_4 tm_{t-1} + (1 - \beta_4) dm_t, \\ tv_t &= \beta_5 tv_{t-1} + (1 - \beta_5) dv_t. \end{aligned} \quad (9)$$

Here, $(m_0, v_0), (dm_0, dv_0), (tm_0, tv_0)$ are all initialized to 0.

Incorporating Eqs. (7-9) into the TEMA equation (5) gives

$$\begin{aligned} m_{\text{FAME}_t} &= 3m_t - 3dm_t + tm_t, \\ v_{\text{FAME}_t} &= 3v_t - 3dv_t + tv_t. \end{aligned} \quad (10)$$

Our final parameter update equation is then

$$\theta_t = \theta_{t-1} - \alpha \cdot \frac{m_{\text{FAME}_t}}{\sqrt{v_{\text{FAME}_t} + \epsilon}}. \quad (11)$$

In our experiments, we assigned the following values to the hyper-parameters: $\alpha = 0.001$, $\beta_1 = 0.9$, and $\beta_2 = 0.999$. These values are commonly used in Adam, SGD + Momentum, etc. We also selected $\beta_3 = 0.3$, $\beta_4 = 0.5$, $\beta_5 = 0.8$, and $\epsilon = 1e - 8$. These values were selected empirically because they provided the best results.

C. Convergence Analysis

To demonstrate the convergence of the proposed FAME algorithm, we begin by establishing a mathematical framework. Let $d \in \mathbb{N}$ represent the number of parameters in the function $F : \mathbb{R}^d \rightarrow \mathbb{R}$ that we aim to optimize. In the domain of machine learning, F embodies the complete training objective function, and optimization algorithms are employed to locate critical points within F . Specifically, our focus lies on optimization techniques that expand upon the classical Gradient Descent (GD) algorithm by integrating a heavy-ball style momentum parameter [18]. These algorithms exhibit a continuously diminishing step size from an initial finite step, leading to a monotonically decreasing process [7]. This behavior underscores their progression towards convergence.

Let us assume several constraints: $0 \leq \beta_5 \leq \beta_3 \leq \beta_1 \leq 1$ and $0 \leq \beta_4 \leq \beta_2 \leq 1$, along with the condition $\beta_1 \leq \beta_2$, and a non-negative value for α .

According to Algorithm 1, we define three sequences, $m_i, v_i, \theta_i \in \mathbb{R}^n$, where n denotes the dimension of the parameter space. Given an initial point $\theta_0 \in \mathbb{R}^n$ and setting $m_0 = v_0 = 0$, we proceed under three primary assumptions:

- The loss function F is bounded below by an arbitrary function F^* for any point $\forall \theta \in \mathbb{R}^n : F^*(\theta) \leq F(\theta)$.
- The loss function, concerning the max-norm (l_∞), is uniformly and surely bounded: $\forall \epsilon > 0 \exists r > \epsilon \forall \theta \in \mathbb{R}^n : \|\nabla F\|_\infty \leq r - \epsilon$.
- The loss function maintains L-Lipschitz continuity concerning the l_2 -norm: $\forall \theta, \zeta \in \mathbb{R}^n : \|\nabla F(\theta) - \nabla F(\zeta)\|_2 \leq L\|\theta - \zeta\|_2$.

For a specific number of iterations $N \in \mathbb{N}$, we introduce τ as a random index ranging from $\{0, \dots, N - 1\}$, where $\forall i \in \mathbb{N} : i < N, P[\tau = i] \propto 1 - \beta_1^{N-i}$. This implies that for $\beta_1 = 0$, τ is uniformly sampled, while higher orders approaching zero lead to fewer samples in later iterations. This stratagem aims to limit the expected squared gradient norm at iteration τ .

For $N > \beta_1/(1 - \beta_1) \in \mathbb{N}$, the following inequality holds:

$$\begin{aligned} \|\nabla F(\theta_\tau)\|^2 &\leq \\ 2r\sqrt{N} \frac{F(\theta_0) - F^*}{\alpha(N - \beta_1/(1 - \beta_1))} + \\ \frac{\sqrt{N}}{N - \beta_1/(1 - \beta_1)} \ln(1 + \frac{Nr^2}{\epsilon}) & \left(\alpha nrL + \frac{12dR^2}{1 - \beta_1} + \frac{2\alpha^2 dL^2 \beta_1}{1 - \beta_1} \right) \end{aligned} \quad (12)$$

Continuing with Algorithm 1 (lines 4-12), we can split the proof into two cases:

- When $\beta_3 = \beta_5 = \beta_4 = 0$, the algorithm adopts the form $\theta_t = \theta_{t-1} - \alpha \frac{m_t}{v_t}$, akin to the ADAGRAD algorithm, known for convergence [19].
- For $\exists j \in \{3, 4, 5\} : \beta_j > 0$, dm_t, tm_5, dv_t , and tv_t depend on m_t and v_t , converging at some point following the first case. Thus, a $\delta \in \mathbb{N}$ emerges with $\epsilon^* > 0 \in \mathbb{R}$ such that $\|\psi_\delta - \psi_{\delta-1}\|_2 \leq \epsilon^*$ for $\psi \in \{dm, tm, dv, tv\}$. Consequently, beyond this interaction (δ), the update rule transforms into $\forall t > \delta : \theta_t = \theta_{t-1} - \alpha \frac{m_t + c_1}{v_t + c_2}$, with $c_1, c_2 \in \mathbb{R}^n$. This update rule can be upper-bounded by a constant $c_3 \in \mathbb{R}^n$, resembling the ADAGRAD, because the adaptive update roughly aligns with the descent direction. Thus, the convergence at $\tau \in \mathbb{N}$ implies subsequent steps being smaller, bounded by ADAGRAD convergence processes from the same initial configuration.

Ultimately, by establishing an upper limit to convergence in the second case, we demonstrate convergence in this scenario as well.

V. EXPERIMENTS

We conducted comprehensive validation experiments to study the capabilities of the proposed FAME optimizer. We analyzed **six diverse benchmarks** using **15 model architectures** with varying complexities for multiple computer vision **tasks**, including detection, classification, and semantic understanding. We compared FAME with **six popular and commonly used optimizers**, namely, SGD + Momentum, Adam, Adagrad, AdamW, AdaBound, and AdaHessian (Table I). For a fair comparison, we adopted **identical initial weights** for all tested optimizers. Additionally, we trained all models from **scratch to highlight the genuine impact of each optimizer** on the learning process, thus, providing valuable insights into the behavior and effectiveness of the specific optimizer. Although this approach may result in slightly reduced accuracy compared to that of an approach that leverages pre-trained models, it enables a thorough evaluation of the performance of the examined optimizers without potential biases from previously learned parameters. Thus, we gain a comprehensive understanding of the capabilities of the optimizer in tackling diverse optimization challenges to assess its reliability in converging toward optimal solutions across various starting points. We also carefully optimized the network performance and conducted an extensive hyper-parameter search to align the chosen parameters with the defaults documented in the literature to **ensure that all the networks were appropriately tuned**.

A. Experimental Data

1) *Simulated Data*: We assessed our new optimizer in a two-dimensional (2D) space containing multiple local minima following the methodology in [20]. All optimizers commenced from the same starting point, and 30 random points were selected. Fig. 2 illustrates that FAME outperforms both Adam and SGD in terms of converging accurately toward the intended minimum, factoring in the depth and proximity to the initial

Optimizer	First Moment	Second Moment	Update Rule
SGD + Momentum	$m_t = \beta_1 m_{t-1} + (1 - \beta_1) g_t$	$v_t = 1$	$\theta_t = \theta_{t-1} - \alpha g_t$
AdaGrad	$m_t = g_t$	$v_t = \beta_2 v_{t-1} + (1 - \beta_2) g_t^2$	$\theta_t = \theta_{t-1} - \alpha \cdot \left(\frac{m_t}{\sqrt{\sum_{i=1}^T g_i g_i + \epsilon}} \right)$
Adam	$m_t = \beta_1 m_{t-1} + (1 - \beta_1) g_t$	$v_t = \beta_2 v_{t-1} + (1 - \beta_2) g_t^2$	$\theta_t = \theta_{t-1} - \alpha \cdot \frac{m_t}{\sqrt{v_t + \epsilon}}$
AdamW	$m_t = \beta_1 m_{t-1} + (1 - \beta_1) g_t$	$v_t = \beta_2 v_{t-1} + (1 - \beta_2) g_t^2$	$\theta_t = \theta_{t-1} - \alpha \cdot \left(\frac{m_t}{\sqrt{v_t + \epsilon}} + \lambda_t \theta_{t-1} \right)$
AdaHessian	$m_t = \frac{(1 - \beta_1) \sum_{i=1}^t \beta_1^{t-i} g_i}{1 - \beta_1^t}$	$v_t = \frac{(1 - \beta_2) \sum_{i=1}^t \beta_2^{t-i} D_t^{(s)^2}}{1 - \beta_2^t}$	$\theta_t = \theta_{t-1} - \alpha \cdot \frac{m_t}{\sqrt{v_t + \epsilon}}$
Our FAME (Adam's m_t, v_t)	$m_{FAME_t} = 3m_t - 3dm_t + tm_t$	$v_{FAME_t} = 3v_t - 3dv_t + tv_t$	$\theta_t = \theta_{t-1} - \alpha \cdot \frac{m_{FAME_t}}{\sqrt{v_{FAME_t} + \epsilon}}$

TABLE I: SUMMARY OF THE FIRST AND SECOND MOMENTS USED IN DIFFERENT OPTIMIZATION ALGORITHMS FOR MODEL UPDATING

position. Of the 30 initial points, FAME exhibited accurate convergence with 90% accuracy, surpassing the performances of SGD and Adam, which achieved accuracies of 83.33% and 76.66%, respectively. This finding demonstrates the robustness of FAME against the higher sensitivity provided by SGD and Adam to initializations.

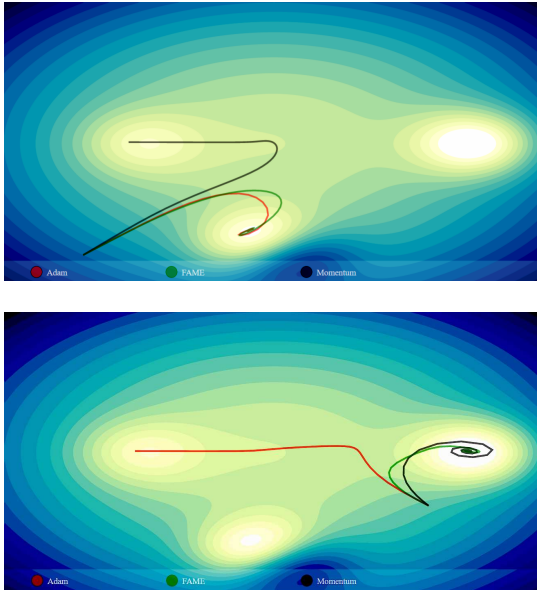


Fig. 2: Simulated data of two-dimensional (2D) space with several local minima. The FAME (green), Adam (red), and SGD + Momentum (black) optimizers are compared. Examples of two different initial points. In both cases, FAME converges toward the correct local minimum and outperforms SGD + Momentum and Adam. In contrast, SGD + Momentum and Adam converge to the suboptimal local minima in the upper image and the lower image, respectively.

2) *Public Benchmarks*: We also tested our proposed FAME on six public benchmarks: CIFAR-10, CIFAR-100 [21], MS-COCO [22], PASCAL-VOC [23], Cityscapes [24], and the large scale ImageNet [25].

B. Implementation Details

For each dataset, we meticulously tuned the hyper-parameters (Table II) and validated them with commonly used values from the literature:

	CIFAR	COCO	PASCAL	City	ImageNet
Batch size	128	128	48	16	128
LR	0.001	0.001	0.0334	0.001	0.001
Momentum	0.94	0.94	0.75	0.9	0.9
WD	0.005	0.005	0.00025	0.0001	0.0001
Warmup	3	3	3	3	3
Epochs	200	250	200	170	40

TABLE II: VALUES OF HYPER-PARAMETERS. LR = LEARNING RATE; WD = WEIGHT DECAY, WARM-UP = WARM-UP EPOCHS

VI. RESULTS

In pursuit of a comprehensive analysis, we computed an array of statistical parameters, including accuracy, mAP (mean Average Precision), precision, recall, and F1-score. This involved evaluating the average and standard deviation across three distinct trials that utilized diverse weight initializations, solidifying the robustness of our assessment.

A. Image Classification

1) *CIFAR-10/CIFAR-100*: Our FAME optimizer exhibits enhanced performance on the CIFAR-10 and CIFAR-100 benchmarks, as seen from the results given in Table III. Across 13 architectures, FAME outperformed both Adam and SGD in 84.6% of the cases. To further establish the capabilities of FAME, we compared it with other optimizers, such as AdaBound, AdamW, AdaGrad, and AdaHessian. The results for the EfficientNet-b3 example in Fig. 3 show that FAME provided the highest and most stable accuracy level, indicating its efficacy. Across *all the tested architectures*, FAME exhibited average improvements of 1.16%, 1.57%, 3.52%, and 16.33% in terms of classification accuracy compared with AdamW, AdaBound, AdaHessian, and AdaGrad, respectively. Figures 3 through 4 highlight a significant observation: **FAME demonstrated consistent and stable performance, without disruptive, noisy fluctuations in accuracy** during training—a stark contrast to the prominent noise disturbances observed with other optimizers. For the EfficientNet-B3 architecture (Fig. 3), FAME exhibits remarkable performance, with the average variance lower than those of the compared optimizers by 29.27%. As illustrated in Fig. 4, when integrated into the RevViT transformer [26], FAME demonstrated a substantial 21.54% reduction in the variance of noisy accuracy values over training epochs relative to Adam and a 15.32% reduction relative to SGD.

2) *ImageNet*: Three random initializations were used to train ResNet-18 (a popular architecture for training ImageNet from scratch). The resulting performance accuracies were calculated to be 0.664 ± 0.002 for the FAME optimizer, 0.656 ± 0.002 for SGD, 0.642 ± 0.003 for Adam, and 0.638 ± 0.004 for AdamW. Furthermore, Fig. 5 highlights various facets of FAME (as a reflection of the observed behavior on CIFAR-100, shown in Fig. 3-4): 1) **Improved Accuracy**-FAME consistently attained the highest accuracy levels among the compared optimizers. 2) **Enhanced Stability**-FAME demonstrates smoother accuracy trends, which are manifested as an average reduction of 5.64% in fluctuations or patterns compared with SGD, Adam, and AdamW. 3) **Accelerated Convergence**-FAME attained good accuracy (e.g., 0.45 in Fig. 4 or 0.6 in Fig. 5) in under half the epochs needed by Adam and SGD (Fig. 4. For example, FAME needs 16 epochs, whereas SGD and Adam required 38 and 40 epochs, respectively. In Fig. 5, 15 epochs are needed instead of 31).

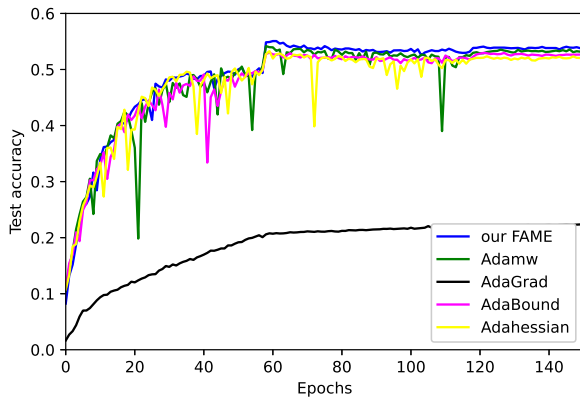


Fig. 3: FAME vs. other optimizers on CIFAR-100. EfficientNet-B3 architecture is trained from scratch.

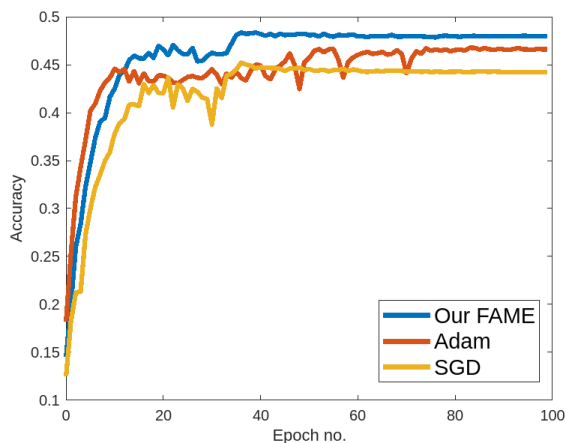


Fig. 4: Comparison of the performance stability of FAME, Adam, and SGD on CIFAR100 using RevVit transformer architecture.

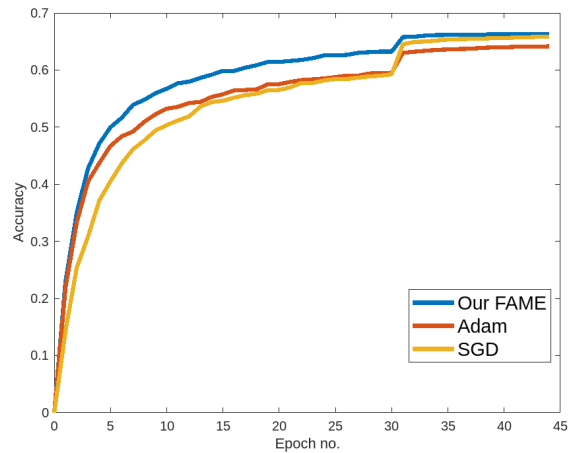


Fig. 5: Classification accuracy on ImageNet (training ResNet-18 from *scratch*).

B. Object Detection

1) *MS-COCO Benchmark*: Table IV presents a comprehensive comparison of performance metrics—mAP@0.5, mAP@0.5:0.95, Precision, Recall, and F1-Score—across various optimization approaches, including Our FAME, SGD, Adam, and AdamW, employed on the YOLOv5-S architecture for the MS-COCO dataset. Analyzing the percentage improvements of our FAME over the other optimizers reveals a significant improvement in object detection accuracy. Our FAME consistently outperforms SGD, Adam, and AdamW across all statistical parameters, showcasing its superior performance in enhancing object detection accuracy on the YOLOv5-S architecture. Specifically, Our FAME exhibits substantial improvements over the other optimizers: an average increase of 14.96% for mAP@0.5, 12.83% for mAP@0.5:0.95, 16.1% for Precision, 15.7% for Recall, and 15.16% for the F1-Score. The significant improvement underlines the superiority of our FAME in optimizing object detection models, reflecting its capability to achieve notably higher accuracy levels compared to widely adopted optimization techniques such as SGD, Adam, and AdamW. The consistent superiority exhibited by our FAME underscores its efficacy and potential in significantly advancing object detection accuracy, positioning it as a robust optimization method in the area of object detection methodologies.

2) *Pascal-VOC Benchmark*: Table V outlines the Mean Average Precision (mAP) for object detection models like Yolov5-s and Yolov5-m, as well as the Area Under the Curve (AUC) for a classification model such as the RevViT vision transformer. Across these models, tasks, and evaluation metrics, it's evident that our FAME is superior to the other optimization techniques—SGD, ADAM, and AdamW—when it comes to achieving higher performance. Specifically, for object detection (as denoted by the mAP scores), our FAME consistently presents superior results. For instance, in the Yolov5-s model, our fame achieves an impressive mAP of 0.812 ± 0.007 , surpassing SGD (0.787 ± 0.007), ADAM (0.651 ± 0.009), and even outperforming ADAMW (0.801 ± 0.009). Similarly, the Yolov5-m model under our FAME attains a high mAP of 0.851 ± 0.006 , which is an average significant

Dataset	Architecture	Our FAME	Adam	SGD + Momentum
CIFAR-10	Resnet18	0.937 ± 0.002	0.924 ± 0.003	0.921 ± 0.006
	EfficientNet-b0	0.492 ± 0.011	0.459 ± 0.015	0.352 ± 0.022
CIFAR-100	EfficientNet-b3	0.538 ± 0.015	0.453 ± 0.017	0.407 ± 0.008
	MobileNet	0.612 ± 0.005	0.601 ± 0.007	0.644 ± 0.011
	DenseNet-121	0.738 ± 0.008	0.664 ± 0.015	0.727 ± 0.011
	DenseNet-201	0.739 ± 0.005	0.742 ± 0.006	0.733 ± 0.006
	SqueezeNet	0.662 ± 0.007	0.651 ± 0.009	0.647 ± 0.011
	Resnet-18	0.723 ± 0.006	0.708 ± 0.008	0.693 ± 0.019
	Resnet-34	0.736 ± 0.006	0.721 ± 0.008	0.698 ± 0.008
	SEResnet-18	0.715 ± 0.009	0.704 ± 0.009	0.692 ± 0.016
	Inception-v3	0.751 ± 0.006	0.743 ± 0.008	0.702 ± 0.015
	WideResnet 40-4	0.719 ± 0.007	0.706 ± 0.009	0.708 ± 0.007
	RevViT transformer	0.483 ± 0.003	0.467 ± 0.007	0.443 ± 0.002

TABLE III: CIFAR-10 AND CIFAR-100 BENCHMARKS. COMPARISON OF CLASSIFICATION ACCURACY (MEAN \pm STD) SUPPLIED BY DIFFERENT OPTIMIZERS ACROSS ARCHITECTURES. **BEST RESULTS FOR EACH ARCHITECTURE ARE BOLDED**. ALL SGD AND ADAM RESULTS ARE COMPARABLE TO THE LITERATURE RESULTS WHEN TRAINING FROM SCRATCH. STD WAS CALCULATED FOR THREE DIFFERENT INITIALIZATIONS.

improvement of 0.07 compared to the alternatives. Furthermore, for object classification (measured by AUC), our FAME again demonstrates its strength. The RevViT model attains an AUC of 0.696 ± 0.006 under our FAME, showcasing superiority against SGD (0.679 ± 0.007), ADAM (0.637 ± 0.009), and still standing out above AdamW (0.671 ± 0.007). Our FAME performance is consistently better across different models, tasks and evaluation metrics (Wilcoxon paired test, $p < 0.005$). This consistency showcases its robustness and reliability in optimizing these models for better object detection and classification tasks.

	Our FAME	SGD	Adam	AdamW
mAP@0.5	0.569 ± 0.003	0.549 ± 0.005	0.265 ± 0.021	0.446 ± 0.013
mAP@0.5:0.95	0.375 ± 0.003	0.352 ± 0.005	0.121 ± 0.021	0.271 ± 0.014
Precision	0.663 ± 0.009	0.658 ± 0.011	0.332 ± 0.013	0.542 ± 0.011
Recall	0.521 ± 0.006	0.427 ± 0.006	0.234 ± 0.019	0.417 ± 0.007
F1-Score	0.583 ± 0.008	0.518 ± 0.012	0.275 ± 0.014	0.471 ± 0.004

TABLE IV: MS-COCO BY YOLOV5-S. STD FOR THREE INITIALIZATIONS. THE RESULTS MATCH THOSE OF TRAINING FROM SCRATCH, AS REPORTED IN LITERATURE

	Our Fame	SGD	ADAM	ADAMW
Yolov5-s (mAP) - Detection	0.812 ± 0.007	0.787 ± 0.007	0.651 ± 0.009	0.801 ± 0.009
Yolov5-m (mAP) - Detection	0.851 ± 0.006	0.828 ± 0.007	0.662 ± 0.011	0.83 ± 0.009
RevViT (AUC) - Classification	0.696 ± 0.006	0.679 ± 0.007	0.637 ± 0.009	0.671 ± 0.007

TABLE V: PASCAL VISUAL OBJECT CLASSES (VOC) DETECTION / CLASSIFICATION. STD WAS CALCULATED FOR THREE INITIALIZATIONS. THE RESULTS MATCH THOSE FOR TRAINING FROM SCRATCH AS REPORTED IN LITERATURE

C. Semantic Segmentation

1) *Cityscapes Benchmark*: Upon analyzing the results, it's evident that our FAME optimization technique achieves a mean IOU score of 0.757 ± 0.005 , outperforming the other three optimizers—SGD, Adam, and AdamW. SGD achieves a mean IOU score of 0.704 ± 0.012 , which is notably lower than that of FAME. Meanwhile, Adam and AdamW perform slightly better than SGD, with scores of 0.743 ± 0.008 and 0.738 ± 0.011 , respectively. However, they still fall short of the performance exhibited by our FAME (Wilcoxon paired test, $p < 0.005$). Moreover, the consistent trend across multiple trials or experiments, as indicated by the narrow standard deviation associated with our FAME technique, emphasizes its stability and reliability in producing superior results compared to the other optimization methods tested.

Our FAME	SGD	Adam	AdamW
0.757 ± 0.005	0.704 ± 0.012	0.743 ± 0.008	0.738 ± 0.011

TABLE VI: CITYSCAPES BENCHMARK. COMPARISON OF CLASSIFICATION MEAN INTERSECTION OVER UNION (IOU) FOR YOLOV5-M. STD WAS CALCULATED USING THREE DIFFERENT INITIALIZATIONS. THE RESULTS MATCH THOSE FOR TRAINING FROM SCRATCH AS REPORTED IN LITERATURE

D. Robustness across Datasets, Architectures, and Weight Initializations

The results in Tables III-VI and Fig. 3-5 show that for 87.5% of the architectures, FAME outperforms all the other optimizers examined in this study, and its performance is comparable with those of the other optimizers for the remaining 12.5% cases. Thus, its high robustness within and across datasets was established. Furthermore, FAME demonstrated a lower standard deviation across the different weight initializations.

E. Ablation Study

- **Effect of high-order EMAs** — The data in Table VII demonstrate the effect of the order of optimizers on

the overall performance accuracy. The results show that increasing the order from simple EMA to DEMA, and then to TEMA, gives additional gains in performance. We also tested the 4th order but it was inferior to TEMA, thus, it was not chosen. In general, adding higher-order terms sacrifices smoothness, while achieving a more aggressive lag reduction. TEMA is a good representative for achieving an adequate balance. In summary, the results unequivocally highlight the superiority of our triple-based FAME, over other high-order EMAs across diverse datasets, tasks, and architectures. It supplies consistently higher accuracy across various tasks emphasizing the potential and reliability of our FAME, compared with the other high-order EMAs.

- **Effect of TEMA on different moments** — Table VIII shows the effects of integrating TEMA on different components of FAME, the 1st and the 2nd moments. The transition from EMA to Partial TEMA highlights the influence of TEMA on estimating m_{FAME_t} exclusively (whereas v_t uses EMA, as in Adam). The shift from Partial TEMA to FAME demonstrates the additional value imparted by TEMA to the accuracy of FAME because TEMA can be extended to estimate both m_{FAME_t} and v_{FAME_t} . The table reveals that integrating TEMA into each moment estimation consistently enhances the overall accuracy of the FAME. The results clearly indicate that our FAME, leveraging both M_{FAME_T} and V_{FAME_T} components, consistently leads to better performance in various evaluation metrics and datasets compared to ADAM (original EMA) and Partial FAME approaches. This showcases the robustness and effectiveness of our FAME in enhancing model optimization, particularly in object detection, classification, and semantic segmentation tasks across different datasets and architectures.

Conclusively, the comprehensive analysis carried out in this ablation study firmly establishes the proposed FAME as a superior optimizer. Demonstrating consistent performance enhancements over other high-order EMAs and even when compared to the integration of the triple-based EMA solely for the 1st moment, these results unambiguously affirm the unmatched efficiency and effectiveness of FAME across a diverse array of datasets and evaluation metrics.

Dataset	Architecture	EMA	DEMA	Our FAME
CIFAR-100	ResNet34	0.721 ± 0.008	0.727 ± 0.006	0.736 ± 0.006
MS-COCO	YOLOv5-n	0.265 ± 0.021	0.317 ± 0.004	0.529 ± 0.003
PASCAL-VOC	YOLOv5-m	0.662 ± 0.011	0.806 ± 0.005	0.851 ± 0.006
Cityscapes	Deeplabv3	0.743 ± 0.008	0.751 ± 0.005	0.757 ± 0.005

TABLE VII: ABLATION-STUDYING THE EFFECTS OF THE OPTIMIZER ORDER

Dataset	ADAM (Original EMA)	Partial FAME	Our FAME
CIFAR-100 (Accuracy)	0.721 ± 0.008	0.729 ± 0.005	0.736 ± 0.006
MS-COCO (mAP)	0.265 ± 0.021	0.504 ± 0.006	0.529 ± 0.003
PASCAL-VOC (mAP)	0.662 ± 0.011	0.829 ± 0.008	0.851 ± 0.006
CityScapes (mean IoU)	0.743 ± 0.008	0.751 ± 0.005	0.757 ± 0.005

TABLE VIII: ABLATION STUDY. "PARTIAL FAME" MEANS USING TEMA FOR M_{FAME_T} ONLY, WHILE "OUR FAME" MEANS USING TEMA FOR BOTH OF M_{FAME_T} AND V_{FAME_T} . CIFAR100: RESNET50, MS-COCO: YOLOV5-N, PASCAL-VOC: YOLOV5-M, AND CITYSCAPES: RESNET50+ DEEPLABV3.

F. Sensitivity to Hyper-parameter Tuning

FAME introduces three new hyper-parameters (β_3, β_4 , and β_5) along with the already existing β_1 and β_2 from Adam. First, we conducted a grid search on β_1 and β_2 for Adam (a specific case of FAME). The most significant accuracy variation among the different sets of hyper-parameters was 10.12%. We then set β_1 and β_2 at their default Adam values of 0.9 and 0.999, respectively. Subsequently, we performed an extensive grid search for the additional FAME parameters: β_3, β_4 , and β_5 . Across the various hyper-parameter configurations, the largest difference in accuracy observed was 3.72%. This trend persisted for alternate datasets (CIFAR-100, ImageNet, Cityscapes, MS-COCO, and Pascal-VOC) within the same hyper-parameter range. Therefore, although the inclusion of extra hyper-parameters slightly enhances the sensitivity, the susceptibility to higher-order parameters remains lower than that of the first-order parameters.

G. Memory Cost and Computational Time

The assessment of memory cost and consumption involves two main aspects. 1) *Epoch-wise Analysis*—In each epoch, our FAME algorithm incurs a modest increase in memory usage, approximately 7%, compared to the traditional ADAM and SGD optimizers. Additionally, the optimization process of FAME introduces a slight increase of approximately 5% in the computational time. 2) *Total Convergence Time*—Despite the slightly longer duration of individual epochs of FAME, its distinct convergence behavior drastically reduces the number of epochs required for satisfactory convergence. This unique finding, as detailed and well supported in the Results section, translates to a considerable reduction in the total analysis time. By adopting FAME as the optimizer, the overall analysis duration can be shortened to about 40% of the time required by ADAM and SGD.

VII. CONCLUSION

This paper introduces FAME, a novel optimizer harnessing the power of high-order Exponential Moving Averages (EMA). FAME, a 3rd-order EMA (i.e., TEMA), draws inspiration from the financial domain. However, unlike the *passive* role

of technical indicators like TEMA in finance, FAME takes an **active** stance by directly influencing optimization and network weights. By **dynamically** engaging in the optimization process, FAME significantly enhances the adaptability of deep learning models. Addressing inherent challenges found in traditional EMA-based optimizers, FAME focuses on addressing issues such as trend identification lagging and effectively managing fluctuations in noisy gradients.

The effectiveness of FAME in overcoming these hurdles is comprehensively demonstrated and well-supported through the extensive experimental results presented in this paper. The validation of FAME's abilities across diverse public benchmarks, computer vision tasks, and learning architectures was conducted. Remarkably, FAME consistently demonstrates superiority across various aspects of model performance, including accuracy, robustness, mitigation of noisy gradient fluctuations, and a reduced number of epochs required for convergence. These advantages stand out prominently when compared against other widely used optimizers examined in this study.

We strongly believe that the great potential of our proposed FAME optimizer, which effectively addresses a fundamental challenge within the core of deep models, holds promise for further research in additional domains. These domains include but are not limited to Natural Language Processing, speech analysis, and various other fields, beyond the confines of computer vision.

REFERENCES

- [1] N. Maheswaranathan, D. Sussillo, L. Metz, R. Sun, and J. Sohl-Dickstein, "Reverse engineering learned optimizers reveals known and novel mechanisms," *CoRR*, vol. abs/2011.02159, 2020. [Online]. Available: <https://arxiv.org/abs/2011.02159>
- [2] H. Robbins and S. Monro, "A stochastic approximation method," *The annals of mathematical statistics*, pp. 400–407, 1951.
- [3] N. Qian, "On the momentum term in gradient descent learning algorithms," *Neural networks : the official journal of the International Neural Network Society*, vol. 12 1, pp. 145–151, 1999.
- [4] M. D. Zeiler, "Adadelta: An adaptive learning rate method," 2012.
- [5] J. Duchi, E. Hazan, and Y. Singer, "Adaptive subgradient methods for online learning and stochastic optimization," *Journal of Machine Learning Research*, vol. 12, pp. 2121–2159, 07 2011.
- [6] T. Tieleman and G. Hinton, "Lecture 6.5—RmsProp: Divide the gradient by a running average of its recent magnitude," COURSE: Neural Networks for Machine Learning, 2012.
- [7] D. P. Kingma and J. Ba, "Adam: A method for stochastic optimization," *arXiv preprint arXiv:1412.6980*, 2014.
- [8] S. J. Reddi, S. Kale, and S. Kumar, "On the convergence of adam and beyond," 2019. [Online]. Available: <https://arxiv.org/abs/1904.09237>
- [9] L. Luo, Y. Xiong, Y. Liu, and X. Sun, "Adaptive gradient methods with dynamic bound of learning rate," *CoRR*, vol. abs/1902.09843, 2019. [Online]. Available: <http://arxiv.org/abs/1902.09843>
- [10] I. Loshchilov and F. Hutter, "Fixing weight decay regularization in adam," 2018. [Online]. Available: <https://openreview.net/forum?id=rk6qdGgCZ>
- [11] Z. Yao, A. Gholami, S. Shen, M. Mustafa, K. Keutzer, and M. Mahoney, "Adahessian: An adaptive second order optimizer for machine learning," in *proceedings of the AAAI conference on artificial intelligence*, vol. 35, no. 12, 2021, pp. 10 665–10 673.
- [12] N. S. Keskar and R. Socher, "Improving generalization performance by switching from adam to sgd," *arXiv preprint arXiv:1712.07628*, 2017.
- [13] N. Landro, I. Gallo, and R. L. Grassa, "Mixing ADAM and SGD: a combined optimization method," *CoRR*, vol. abs/2011.08042, 2020. [Online]. Available: <https://arxiv.org/abs/2011.08042>
- [14] A. Gupta, R. Ramanath, J. Shi, and S. S. Keerthi, "Adam vs. sgd: Closing the generalization gap on image classification," in *OPT2021: 13th Annual Workshop on Optimization for Machine Learning*, 2021.
- [15] A. Maiya, I. Sricharan, A. Pandey, and S. K. S., "Tom: Leveraging trend of the observed gradients for faster convergence," *CoRR*, vol. abs/2109.03820, 2021. [Online]. Available: <https://arxiv.org/abs/2109.03820>
- [16] A. Kolkova, "Indicators of technical analysis on the basis of moving averages as prognostic methods in the food industry," *Journal of Competitiveness*, vol. 10, no. 4, pp. 102–119, 2018.
- [17] P. G. Mulloy, "Smoothing data with faster moving averages," *Technical Analysis of Stocks & Commodities*, 1994. [Online]. Available: <http://technical.traders.com/archive/volume-2014.asp?yr=1994#Jan>
- [18] B. T. Polyak, "Some methods of speeding up the convergence of iteration methods," *USSR computational Mathematics and Mathematical Physics*, 1964.
- [19] A. Defossez, L. Bottou, F. Bach, and N. Usunier, "A simple convergence proof of adam and adagrad," *Machine Learning Research*, 2022.
- [20] E. Dupont, "Optimization algorithms visualization," <https://bl.ocks.org/EmilienDupont/aaf429be5705b219aaaf8d691e27ca87>, 2016.
- [21] A. Krizhevsky, "Learning multiple layers of features from tiny images," *technical report*, pp. 32–33, 2009. [Online]. Available: <https://www.cs.toronto.edu/~kriz/learning-features-2009-TR.pdf>
- [22] T.-Y. Lin, M. Maire, S. Belongie, J. Hays, P. Perona, D. Ramanan, P. Dollár, and C. L. Zitnick, "Microsoft coco: Common objects in context," in *European conference on computer vision*. Springer, 2014, pp. 740–755.
- [23] M. Everingham, S. M. A. Eslami, L. Van Gool, C. K. I. Williams, J. Winn, and A. Zisserman, "The pascal visual object classes challenge: A retrospective," *International Journal of Computer Vision*, vol. 111, no. 1, pp. 98–136, Jan. 2015.
- [24] M. Cordts, M. Omran, S. Ramos, T. Rehfeld, M. Enzweiler, R. Benenson, U. Franke, S. Roth, and B. Schiele, "The cityscapes dataset for semantic urban scene under-

standing,” in *Proceedings of the IEEE conference on computer vision and pattern recognition*, 2016, pp. 3213–3223.

- [25] O. Russakovsky, J. Deng, H. Su, J. Krause, S. Satheesh, S. Ma, Z. Huang, A. Karpathy, A. Khosla, M. Bernstein, A. C. Berg, and L. Fei-Fei, “ImageNet Large Scale Visual Recognition Challenge,” *International Journal of Computer Vision (IJCV)*, vol. 115, no. 3, pp. 211–252, 2015.
- [26] K. Mangalam, H. Fan, Y. Li, C.-Y. Wu, B. Xiong, C. Feichtenhofer, and J. Malik, “Reversible vision transformers,” 2023.

1



Roi Peleg Roi Peleg earned both BSc and MSc degrees in Computer Science from Ariel University (direct path). Roi specialized in the fields of Deep Learning and Computer Vision, focusing on developing cutting-edge strategies especially for deep network optimization. Currently, Roi serves as a Research Assistant, incorporating core ideas of Natural Language Processing (NLP) and Large Language Models (LLMs) for computer vision tasks. Additionally, Roi actively engages in bridging the gap between theoretical advancements and real-world

implementations, introducing innovative solutions to enhance deep models’ performance.



Teddy Lazebnik Teddy Lazebnik received the BSc and MSc degrees in mathematics from Bar Ilan University, in 2016 and 2018, respectively. In addition, Teddy received his PhD degree in mathematics from Ariel University, in 2021. During 2021-2023 he was a post-doctoral fellow at University College London and then joined the Department of Mathematics at Ariel University, in 2023 as an assistant professor. His research interests include mathematical and computational modeling and in particular, he specializes in multi-objective optimization problems and data-

driven models’ development. He has co-authored more than 75 papers.



Assaf Hoogi Assaf Hoogi holds a Ph.D. from the Technion - Israel Institute of Technology, where his research focused on computer vision. Following this, from 2013 to 2018, he served as a postdoctoral fellow at Stanford University, specializing in computer vision and deep learning. His contributions in this domain led to his recognition through the American NCI-NIH Young Investigator Award for advancing computational models in medical imaging. Additionally, one of his papers in 2017 was the most downloaded paper in this research domain. In 2018,

Assaf was a senior researcher in the group led by Professor Michal Irani at the Weizmann Institute. Building on his expertise, in 2021, he furthered his academic journey by joining the computer science department at Ariel University as an assistant professor. His professional trajectory showcases a continuous dedication to advancing computer vision, deep learning, and computational models.